Journal of Clinical and Translational Research 2024; 10(5): 269-282

Journal of Clinical and Translational Research

Journal homepage: http://www.jctres.com/en/home

ORIGINAL ARTICLE

A broad appraisal of decompression-induced physiological stress in different simulated dive profiles

Sergio Rhein Schirato[1]*, Ingrid El-Dash[1], Vivian El-Dash[1], Bruna Bizzarro[2], Alessandro Marroni[3], Massimo Pieri[3], Danilo Cialoni[3,4], Jose Guilherme Chaui-Berlinck[1]

[1]Department of Physiology, Biosciences Institute, University of São Paulo, São Paulo, Brazil, [2]Peter Murányi Experimental Research Center, Albert Einstein Hospital, São Paulo, Brazil, [3]DAN Europe Research Division, Roseto Degli Abruzzi, Italy, [4]Environmental Physiology and Medicine Laboratory, Department of Biomedical Sciences, University of Padova, Padova, Italy

ARTICLE INFO

Article history:
Received: May 30, 2024
Accepted: August 26, 2024
Published Online: October 3, 2024

Keywords:
Decompression
Decompression sickness
Immune system activation
Microparticles
Decompression profiles

**Corresponding author:*
Sergio Rhein Schirato
Department of Physiology, Biosciences Institute, University of São Paulo, São Paulo, Brazil. Email: sergio.schirato@gmail.com

ABSTRACT

Background: The present study was designed to observe if different decompression profiles, calculated as a function of tissue supersaturation during ascent, would result in significantly different outcomes, measured through different physiological stress indicators, even in the absence of symptoms of decompression sickness.
Aim: The aim of this study was to evaluate if simulated decompression profiles would affect the immune system, oxidative stress indicators, and heart rate variability.
Methods: A total of 23 volunteers participated in two different experimental protocols in a dry hyperbaric chamber. These simulated dives comprised two different compression–decompression arrangements with the same maximum pressure and duration but different decompression profiles.
Results: The shallow decompression profile with shorter deeper stops and longer shallow stops presented an increase in the standard deviation of the normal-to-normal R-R interval (a wide indicator of overall variability); the deep decompression profile with longer deeper stops and shorter shallow stops did not exhibit such increase. The shallow decompression profile resulted in an increase in neutrophil count and its microparticles (MPs), but no changes were observed for platelet count and its MPs, as well as for endothelial-derived MPs. In contrast, the deep decompression profile resulted in no changes in neutrophil count and its MPs, but a decrease in platelet count along with an increase in MPs from both platelets and endothelial cells. The observed difference might be related to different levels of decompression-related activation of immune system responses and oxidative processes triggered by different levels of inert gas supersaturation upon surfacing.
Conclusion: From previous results and literature data, we present a tentative schematic of how the velocity of ascent would trigger (or not) pro-inflammatory and immune system responses that could ultimately lead to the development of decompression sickness.
Relevance for patients: Increasing safety in exposure to hyperbaric environments and subsequent decompression by evaluating individual physiological responses to the process.

1. Introduction

Exposure to hyperbaric environments and subsequent decompression has been associated with many physiological alterations, which may culminate in decompression sickness. This condition can manifest itself through a variety of symptoms [1], ranging from joint and/or musculoskeletal pain [2], to cardiovascular and neurological impairment and, ultimately, death. Historically, studies related to decompression have adopted a binary approach in regard to decompression sickness [3], separating symptomatic and asymptomatic events. There is, however, a huge spectrum of possible physiological alterations between these two extremes, to which probabilities of decompression sickness

DOI: https://doi.org/10.36922/jctr.24.00021

occurrence are likely to be associated, based on individual responses.

The present study was designed to observe if different decompression techniques would result in significantly different outcomes, measured through different physiological stress indicators, even in the absence of decompression sickness symptoms. For decades, there has been an ongoing debate about how ambient pressure reduction should be conducted in non-saturation dives [4], i.e., whether the reduction of the ambient pressure should start earlier or later in the decompression phase. Dissolved gas models, based on John S. Haldane's tables [1] and later developed by many others, were, over time, partially replaced by decompression algorithms based on the control of bubble formation and growth, including, among others, the varying permeability model developed by Yount [5], causing the speed in ambient pressure reduction, to start earlier in the decompression phase of the dive, i.e., requiring divers to start decompression stops deeper in the water column.

Given the low overall incidence of decompression sickness, there are little scientific data available to support or reject any decompression algorithm. However, there is a widespread belief that including deeper stops in decompression schedules reduces the physiological stress during ascent and the risk of decompression sickness. Conversely, some studies suggest that slower ascents are related to higher counts of bubbles upon surfacing [6]. Nevertheless, whether these counts translate to a higher probability of decompression sickness remains debated [7]. In one of the largest studies comparing the incidence of decompression sickness in bubble-based models versus dissolved gas-based models (derived from Haldane's work), the United States Navy Experimental Diving Unit [4] concluded that decompression schedules with deep stops had a higher incidence of decompression sickness than those with shallower decompression stops.

These findings could be attributed to the different supersaturation observed in the tissues with slower gas kinetics upon surfacing [4]. During deeper decompression stops, these tissues are not yet saturated and continue to absorb gas from the blood [8]. This opposes the purposes of these stops and may aggravate the stress caused by decompression [4].

Besides the well-documented appearance of bubbles, activation of the immune system and small particle (microparticles [MPs] or microvesicles) formation have been suggested to play an important role in decompression sickness [9-11]. Hence, decompression sickness is not merely a physical or mechanical problem, but instead the result of a complex biochemical process. MPs, shed by different cells in a regulated manner and carrying various nuclear components of their originating cells, such as RNA and DNA, are involved in cell signaling and communication [12]. Different studies have identified them as markers of inflammatory diseases [12], and variations in their levels and their cells of origin have been linked to a range of diseases and inflammatory processes [13,14]. During decompression, or probably even earlier, immune system activation and oxidative stress occur. A recent study found that exposure to high-pressure environments, even in the absence of decompression, is sufficient to increase the production of MPs carrying interleukin-1β [15], a cytokine involved in inflammatory responses. The mechanism behind MP formation has been linked to high inert gas pressure, which induces singlet oxygen formation. This toxic free radical is generated through a cycle involving actin S-nitrosylation, nitric oxide (NO) synthase-2, and nicotinamide adenine dinucleotide phosphate (NADPH) oxidase activation [16]. NADPH oxidase, activated by neutrophils, generates reactive oxygen species (ROS) through its heme enzyme, myeloperoxidase (MPO) [17]. ROS production by activated granulocytes and potentially by other cells is part of an orchestrated physiological first response of the immune system to potential aggressors. Therefore, it is expected that higher expressions of MPO are linked to the generation of ROS, leading to MP production.

Another expected physiological alteration related to decompression is heart rate variability (HRV). Recently published studies reported changes in HRV after exposure to hyperbaric environments [18,19]. HRV is defined as the undirected changes in the interval between successive normal-to-normal heartbeats (triggered by the sinus node, excluding extrasystoles) [20], which results from the balanced action of the sympathetic and the parasympathetic branches of the autonomic nervous system (ANS) [20] as well as other non-neural sources of variation.

HRV is commonly studied in the time and frequency domains, and occasionally through the application of non-linear methods [20]. Different HRV indicators have been associated with sympathetic or parasympathetic activity. For many years, it was believed that the low frequency (LF) bandwidth of the HRV spectrogram (a frequency domain indicator) was associated with sympathetic activity, while the high frequency (HF) band was related to the parasympathetic branch of the ANS [20]. In reality, the association between a given bandwidth and one specific branch of the ANS is not so well-defined, and there are probably other factors contributing to the process. HF is highly impacted by respiratory pattern [20], with a response time akin to the parasympathetic response time of the sinoatrial node. The LF band is associated with blood pressure control loops, supporting an association with sympathetic activity [20]. However, experimental evidence indicates that both branches of the ANS play a role in both LF and HF power. A reduction in HRV has been reported in several cardiological and non-cardiological diseases, ranging from diabetes to renal failure [21]. A reduction in HRV, when analyzed in the frequency domain, has also been associated with inflammatory processes in multiple studies [21,22].

Given the clear role of inflammatory processes and immune responses in compression and subsequent decompression processes, studying HRV in this context could provide important insights into the underlying physiological processes and potential outcomes of hyperbaric exposure. As different decompression protocols alter the dynamics of gas absorption and release by tissues and, consequently, the physiological stress sustained by divers, we hypothesized that profiles with deep stops and those with shallow stops would result in distinct changes in HRV.

DOI: https://doi.org/10.36922/jctr.24.00021

2. Methods

2.1. Study participants

The present study was undertaken in healthy individuals, all trained divers, experienced in the experimental profiles utilized. The volunteers provided written informed consent. The ethical committee of the Biosciences Institute of the University of Sao Paulo approved the experimental protocol (CAAE #91231618.6.0000.5464), and all experiments were performed in accordance with relevant guidelines and regulations.

Briefly, a total of 23 male divers participated in this study. Female volunteers were not accepted to avoid the potential effects of neurovegetative changes due to the menstrual cycle [23]. Two volunteers participated in only one experiment and were released from the second due to medical conditions not related to diving. No decompression sickness symptoms were observed during the experimental dives. Table 1 summarizes the anthropometric data of the study population.

2.2. Simulated dives

Experiments involving exposure compression and subsequent decompression were conducted at the Centro Hiperbárico Paulista (São Paulo Hyperbaric Center), Indaiatuba, São Paulo, Brazil, under the supervision of a trained physician. Each volunteer underwent two different trials, each one with the same maximum depth and bottom time. Decompression schedules were created to simulate different decompression profiles with similar total decompression times. Each trial was performed in the morning, at the same time of the day. Divers were requested to rest for at least 30 min before the start of the experiment, and the interval between the experiments was at least 7 days for each volunteer to minimize any carry-over effect [24]. The experiments executed were performed using electronically controlled closed-circuit rebreathers.

2.3. Simulated dive profiles

The diluent gas mix consisted of 18% oxygen, 45% helium, and 37% nitrogen. Rebreathers were set to keep the oxygen pressure at 121 kPa (1.2 ATA; total pressure: Gauge plus 0.93 atm of surface pressure) throughout the dive, raising the oxygen pressure to 141 kPa (1.4 ATA) at 162 kPa (6 meters of seawater [msw]). The bottom pressure was 638 kPa (53 msw) and the time required to reach this pressure was 20 min. The divers were kept at the simulated bottom for an additional 15 min. Subjects were decompressed at a rate of 9 msw/min until the first decompression stop was reached. The dive profiles are detailed in Table 2.

2.4. Electrocardiographic (ECG) data

ECG records were obtained using superficial electrodes in a modified CM5 thoracic positioning. Data were collected while the subjects were seated in a comfortable position using the MP36 system (BIOPAC Systems, Inc., United States of America [USA]), set up at AHA configuration, with 0.05 and 100 Hz as low and high pass filters, respectively, and a sampling rate of 1000 Hz.

Table 1. Study population characteristics

Parameter	Value
Age (years)	44.18±6.77
Weight (kg)	87.82±13.47
Height (cm)	180.32±8.27
Body mass index	27.03±3.90

Note: Data are presented as the mean±standard deviation.

Table 2. Simulated dive profiles

Decompression profile	Depth (msw)	Time (min)	Breathing loop, PO_2 (ATA)
Deep	53	15	1.2
	27	1	1.2
	24	1	1.2
	21	2	1.2
	18	2	1.2
	15	3	1.2
	12	4	1.2
	9	5	1.2
	6	22	1.4
Shallow	53	15	1.2
	21	2	1.2
	18	2	1.2
	15	3	1.2
	12	4	1.2
	9	6	1.2
	6	26	1.4

Abbreviation: msw: Meters of seawater; PO_2: Partial pressure of oxygen.

There were two phases of continuous data collection: (i) a 30-min pre-dive period to establish the baseline condition for each volunteer; and (ii) a 30-min post-dive reading that was initiated 30 min after the end of the dive. This protocol was adopted due to previous observations that the magnitude of HRV changes tends to be higher in the 2nd half-hour post-decompression. Interestingly, it is well-documented that venous gas bubble counts tend to take approximately the same amount of time to reach a peak [24].

ECG recordings were converted into R-R intervals. The R-R time series was then subdivided into non-overlapping windows of 256 consecutive R-R intervals. Subsequently, the following estimators of HRV were obtained from each window (as detailed by the task force of the European Society of Cardiology and the North American Society of Pacing and Electrophysiology [20]):

(i) Time domain:
- R–R interval
- Standard deviation of the normal-to-normal R-R interval (SDNN)
- The square root of the mean squared differences of successive R-R intervals (RMSSD).

(ii) Frequency domain:
- Fast Fourier transform, to obtain the power spectrum density [20], which was subsequently divided into:
  1. Ultra-LF: 0.01 – 0.04 Hz (not relevant to this study due to the relatively short ECG recording intervals)

DOI: https://doi.org/10.36922/jctr.24.00021

2. LF: 0.04 – 0.15 Hz
3. HF: 0.15 – 0.4 Hz

As the size of the time series tends to infinity, the variance and the total power of the spectrum converge to each other, for this reason, in the present study, the power of a given power spectrum density was approximated by SDNN squared.

2.5. Blood samples

Venous blood was collected from an antecubital arm vein by a trained phlebotomist before and after each (simulated) dive. The following variables were measured: red blood cells, hemoglobin, hematocrit, neutrophils, platelets, immunophenotyping, and MPs for quantification through flow cytometry. The samples were collected using Cyto-Chex BCT tubes (Streck, INC, USA).

Blood samples were drawn immediately before the experiment and 1 h after the end of decompression. Hemograms were performed immediately after collection at the hyperbaric center. Immunophenotyping was performed up to 3 days after the blood collection.

2.6. Flow cytometry

Immunophenotyping was performed using 16-color FACSFortessa™ (Becton & Dickinson Company©, BD, USA) and the manufacturer's acquisition software.

Annexin binding buffer and the following antibodies were purchased from Biolegend (United States of America [USA]): fluorescein isothiocyanate (FITC)-conjugated anti-annexin V, FITC-conjugated anti-human MPO, allophycocyanin (APC)-conjugated anti-human CD41, PerCF594-conjugated anti-human CD14, PerCP-conjugated anti-human CD235, Pacific Blue-conjugated anti-human CD31, AF700-conjugated anti-human CD66b, and APC-conjugated anti-human CD19. In addition, live/dead V-500-conjugated anti-human was used to identify the dead cell population. Immunophenotyping was conducted using flow cytometry to evaluate the population of granulocytes (CD 16+/CD66b+) among live cells. This included evaluating the percentage of granulocytes expressing MPOs on its surface (MPO%) and mean fluorescence intensity of MPO (MPO MFI) as indicators of neutrophil activation. The strategy used in this analysis and the hierarchy of the gates are described in [19].

For MP acquisition and processing, blood was centrifuged at 1500 g for 5 min [25]. The supernatant was centrifuged at 15,000 g for 30 min to pellet the few remaining platelets and cell debris. These samples were then frozen at −80°C, allowing all samples to be analyzed on the same day. MPs were stained with annexin V and analyzed as described in [26]. We define MPs as annexin V-positive particles with diameters up to 1.0 µm. Gates were set to include particles with 0.3 – 1.0 µm diameters, with the exclusion of background corresponding to debris, which is usually present in buffers. Detergent Triton X (Sigma-Aldrich, USA) was used as a control, as MPs are expected to disintegrate in its presence.

Each sample analysis was performed using the software FlowJo Treestar© (FlowJo, Becton & Dickinson Company©, BD, USA) at the Center for Experimental Research of the Hospital Albert Einstein.

2.7. Decompression schedules

All decompression schedules were defined using the ZHL-16b algorithm, calculated through a script written in R language. The compartment half-time for nitrogen and helium was set to the original values published by Bühlmann [2]. At the end of the experiment, maximum supersaturation pressures for each compartment were adjusted by multiplying the intercept a of the linear equations to limit the compartment j supersaturation for a given ambient pressure P_{amb} (in the format $P_{\max j} = \frac{P_{amb}}{bj} + a_j$) by 0.85 and 0.65. The factor b_j was adjusted to calculate stops at 0.20 and 0.45 of the original pressure limits provided by Bühlmann's values for the deep and shallow decompression profiles, respectively,

Compartment on-gassing and off-gassing were calculated through the application of the following differential equation:

$$\frac{dP_j}{dt} = k_j \left(P_A - P_j\right) \quad \text{(I)}$$

where P_j is the pressure of inert gas in compartment j, P_A is the alveolar (inspired) pressure of inert gas, and k_j is the inverse of the half-time of the compartment multiplied by the natural logarithm of 2 ($k_j = ln2\ t_{\frac{1}{2}j}^{-1}$). Solving Equation I would yield:

$$P_j(t) = P_{0,j}\ e^{-k_j\ t} + P_A\ \left(1 - e^{-k_j\ t}\right) \quad \text{(II)}$$

where $P_{0,j}$ is the initial pressure of inert gas in compartment j at the time of a change in the inspired gas and/or hydrostatic pressure [23].

2.8. Statistical analysis

Differences between pre- and post-dive data were determined using Student's t-test, provided that the data followed a normal distribution, as confirmed by the Shapiro–Wilk test. When normal distribution was not confirmed, a non-parametric permutation test with 10,000 simulation rounds was performed to determine the p-value [27]. The limit of significance was set at 0.05 (i.e., $p < 0.05$). Data provided in this study are presented as the mean ± standard error or mean ± standard deviation, as specified accordingly. All data analyses were conducted using scripts implemented in MATLAB (MathWorks Inc., USA) and R.

2.9. Clustering analysis

An unsupervised algorithm for clustering was used to identify subgroups within the dataset. The K-means algorithm with K = 2 (i.e., two different decompression profiles used in the study) was applied to each set of training data, minimizing the distance J, defined by:

$$J = \sum_{i=1}^{k} \sum_{j=1}^{s} \| x_{k,h} - M_j\ ^2 \| \quad \text{(III)}$$

Data were normalized according to Equation IV and then used to create the normalized matrix:

DOI: https://doi.org/10.36922/jctr.24.00021

$$x_{k,h} = \frac{x'_{k,h} - \min(x'_h)}{max(x'_h) - \min(x'_h)} \quad \text{(IV)}$$

Where $x_{k,h}$ is the normalized variable.

A confusion matrix was computed to assess the accuracy of the algorithm in attributing the results observed for each volunteer to the respective decompression profile.

3. Results

3.1. HRV

An overall increase in variability was observed for both profiles. For the deep decompression profile, the frequency domain indicators LF, total LFs (very LF + LF), and HF increased but were not statistically significant. LF as a fraction of HF and total variability, respectively, and HF as a fraction of total variability did not exhibit significant changes. In the time domain, RMSSD was significantly increased in post-dive values. SDNN also displayed a tendency to increase, though not statistically significant (Table 3).

The shallow decompression profiles also displayed an overall increase in variability. In the frequency domain, HF and LF as a fraction of HF demonstrated a significant increase. In the time domain, SDNN and RMSSD post-dive values significantly increased (Table 4).

The shallow decompression profile resulted in an increase in post-dive variability, observed from SDNN (i.e., from 42.66 ± 2.35 to 49.43 ± 4.02; p = 0.039), while the deep decompression profile did not exhibit a significant change (i.e., SDNN: 43.39 ± 2.29 – 46.3 ± 3.84; p = 0.21). Both profiles displayed a significant increase in the RMSSD index, i.e., from 19.09 ± 1.43 to 25.4 ± 3.19 (p = 0.014) in the shallow decompression profile and from 20.62 ± 1.73 to 24.7 ± 2.61 (p = 0.003) in the deep decompression profile (Figure 1). Both pre-dive baseline SDNN and RMSSD values were not statistically different between profiles (Figure 2).

In addition, a comparison between post-dive SDNN and RMSSD divided by their pre-dive values (respectively, defined as SDNN and RMSSD ratios) is displayed in Figure 3. Notably, the shallow decompression profile generated higher values, though the difference was not statistically significant.

Table 3. Heart rate variability for the deep decompression profile

Parameter	Pre-dive	Post-dive	p
LF (ms^2)	418.00±77.37	545.01±89.09	0.071
Total LFs (ms^2)	176.18±96.73	151.51±132.61	0.060
HF (ms^2)	77.93±15.74	124.50±21.59	0.696
LF/HF ratio	7.31±1.16	8.79±2.00	0.145
LF as a ratio of total variability	0.20±0.02	0.24±0.03	0.059
HF as a ratio of total variability	0.03±0.00	0.04±0.01	0.097
RMSSD	20.62±1.73	24.76±2.61	0.003
SDNN (ms)	43.39±2.29	46.31±3.84	0.217

Note: Data arepresented as mean±standard error.
Abbreviations: LF: Low frequency; HF: High frequency; SDNN: Standard deviation of the normal-to-normal R-R interval; RMSSD: Root mean squared differences of successive R-R intervals.

Table 4. Heart rate variability for the shallow decompression profile

Parameter	Pre-dive	Post-dive	p
LF (ms^2)	468.04±67.46	647.86±133.48	0.057
Total LFs (ms^2)	663.60±88.75	555.03±171.94	0.050
HF (ms^2)	61.99±9.46	96.15±19.51	0.025
LF/HF ratio	8.97±1.03	9.59±1.43	0.031
LF as a ratio of total variability	0.25±0.03	0.23±0.03	0.138
HF as a ratio of total variability	0.03±0.00	0.03±0.01	0.232
RMSSD	19.09±1.43	25.43±3.19	0.014
SDNN (ms)	42.66±2.35	49.43±4.02	0.039

Note: Data arepresented as mean±standard error.
Abbreviations: LF: Low frequency; HF: High frequency; SDNN: Standard deviation of the normal-to-normal R-R interval; RMSSD: Root mean squared differences of successive R-R intervals.

3.2. Blood assay

Red blood cells, hematocrit, hemoglobin, neutrophils, and platelet counts were different between pre- and post-dive measurements. A statistically significant reduction in red blood cells was observed in the deep decompression profile, while the reduction observed in the shallow decompression profile was not significant (Figure 4).

Similarly, a statistically significant reduction in hemoglobin was observed in the deep decompression profile, while the reduction in hemoglobin in the shallow decompression profile was not significant (Figure 5).

Both profiles reported platelet count reduction post-dive, but the reduction was only statistically significant for the deep decompression profile (Figure 6).

Meanwhile, the neutrophil count increased post-dive in both profiles but was only significant in the shallow decompression profile (Figure 7).

Finally, post-dive hematocrit values were slightly lower than pre-dive values in both decompression profiles, but no statistically significant differences between pre- and post-dive values or between profiles were observed.

3.3. Flow cytometry

Pre- and post-dive neutrophil-, endothelium-, and platelet-derived MP counts in the deep and shallow decompression profiles are displayed in Figures 8 and 9, respectively, and detailed in Tables 5 and 6, respectively. These results are consistent with the increased post-dive neutrophil count (Figure 7).

3.4. Clustering analysis

The clustering algorithm was able to distinguish between the decompression profiles using values from the pre- and post-dive ratios of HRV indicators, blood assay, and MP production with an accuracy of 0.68 (confidence interval [CI]: 0.4817 – 0.8204; p = 0.07). Figure 10 presents the two clusters of results created by the algorithm.

4. Discussion

In recent years, numerous studies have demonstrated that decompression sickness is a multifactorial condition that involves the activation of many biochemical pathways, and its mechanisms

DOI: https://doi.org/10.36922/jctr.24.00021

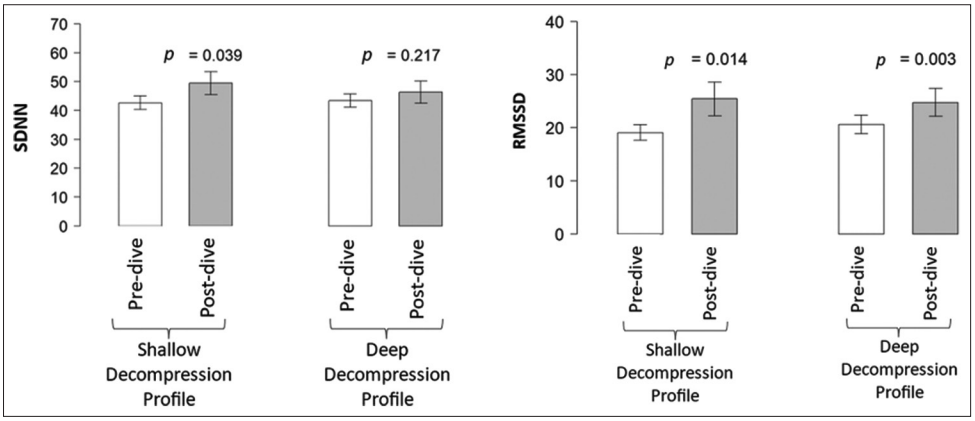

Figure 1. Mean SDNN (left) and RMSSD (right) of pre- and post-dive data for each decompression profile (n = 23)
Abbreviations: SDNN: Standard deviation of the normal-to-normal R-R interval; RMSSD: Square root of the mean squared differences of successive R-R intervals

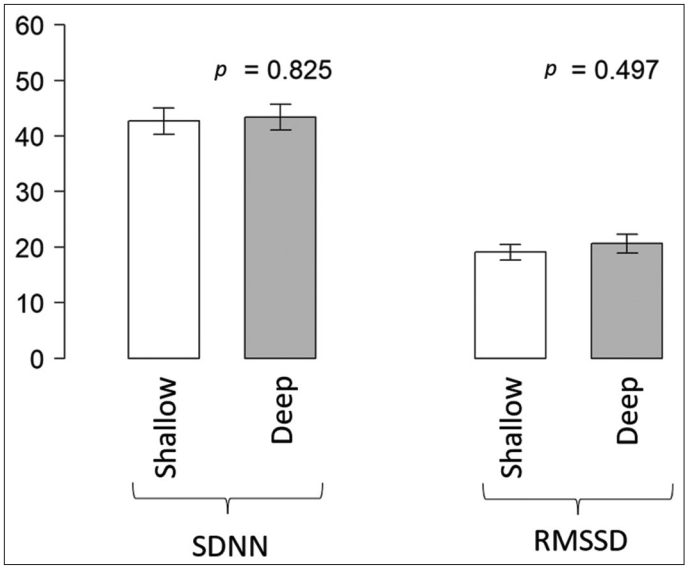

Figure 2. SDNN and RMSSD pre-dive data comparison between the shallow and deep decompression profiles (n = 23)
Abbreviations: SDNN: Standard deviation of the normal-to-normal R-R interval; RMSSD: Square root of the mean squared differences of successive R-R intervals

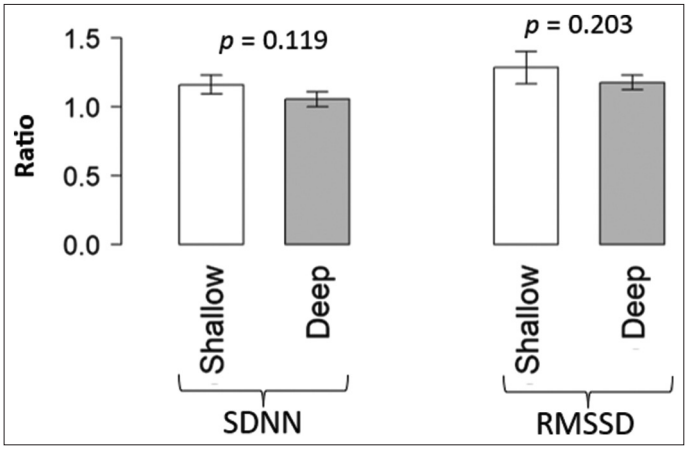

Figure 3. Comparison of SDNN and RMSSD ratios for both shallow and deep decompression profiles (n = 23)
Abbreviations: SDNN: Standard deviation of the normal-to-normal R-R interval; RMSSD: Square root of the mean squared differences of successive R-R intervals

remain not fully understood [28,29]. The present study aims to evaluate possible associations between different levels of inert gas supersaturation in different theoretical compartments and their respective outcomes, in terms of HRV alterations, inflammation, and oxidative processes. Clustering analysis demonstrated that the outcomes of the different profiles can be differentiated with reasonable accuracy, despite the relatively small sample size, supporting the notion that they are distinct. The utilization of HRV is based on its well-established negative correlation with inflammation and immune system activation [30]. Recent studies have reported that hyperbaric exposure and subsequent decompression are associated with HRV changes [31,32]. In a previous work [18], we observed an increase in the LF band post-decompression from 45 msw-simulated dives. Here, a similar pattern is observed (Tables 5 and 6), indicating that decompression generally increases HF, SDNN, and LF.

Other studies also reported that immersion and inspiration of higher partial pressures of oxygen are associated with HRV changes [33], occurring even before ambient pressure reduction, during decompression, or ascent in self-contained breathing apparatus diving. It is plausible that the general post-dive increase in HRV observed in this and other studies is related to hyperoxia, which is commonly linked to exposure to hyperbaric environments where inspired oxygen pressures are typically at 1.0 – 1.2 ATA.

The observed changes in the total LF band could be associated with changes in the baroreceptor activity. LF is linked to baroreflex function, as previous studies demonstrated that carotid sinus stimulation increases LF power in individuals with normal baroreflex function, but not in those with impaired baroreflex sensitivity [34,35]. In addition, LF has been negatively correlated with endothelial function [22]. The ANS and the endothelium work together to maintain vascular tone. There is a tonic balance between the release of vasodilating factors from the endothelium and vasoconstricting factors

DOI: https://doi.org/10.36922/jctr.24.00021

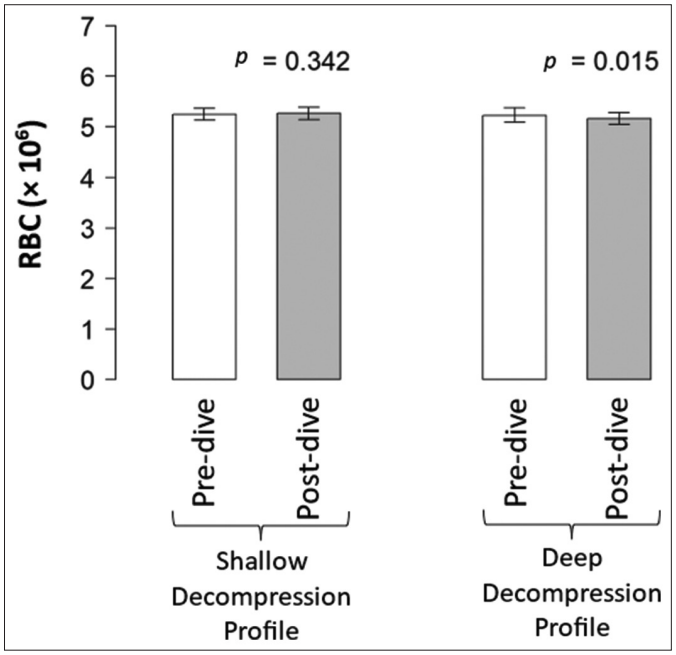

Figure 4. Red blood cell count (mean ± standard deviation) for both shallow and deep decompression profiles (n = 17). In the shallow decompression profile, the pre-dive mean count was $5.25 \times 10^6 \pm 0.48 \times 10^6$, while the post-dive mean count was $5.23 \times 10^6 \pm 0.57 \times 10^6$. In the Deep Decompression Profile, the pre-dive mean count was $5.26 \times 10^6 \pm 0.48 \times 10^6$, while the post-dive mean count was $5.16 \times 10^6 \pm 0.45 \times 10^6$

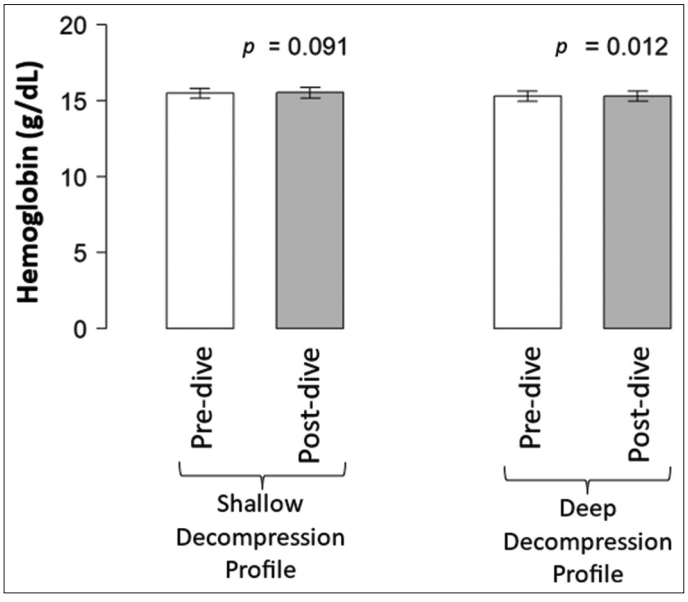

Figure 5. Hemoglobin levels for the shallow and deep decompression profiles (n = 17). Both profiles have a pre-dive mean hemoglobin level of 15.5 g/dL and a post-dive mean hemoglobin level of 15.3 g/dL. The difference in standard deviation for both profiles resulted in statistically significant differences. For the shallow decompression profile, the pre-dive standard deviation was 1.34 g/dL and the post-dive standard deviation was 1.42 g/dL; for the deep decompression profile, the pre- and post-dive standard deviations were 1.40 g/dL

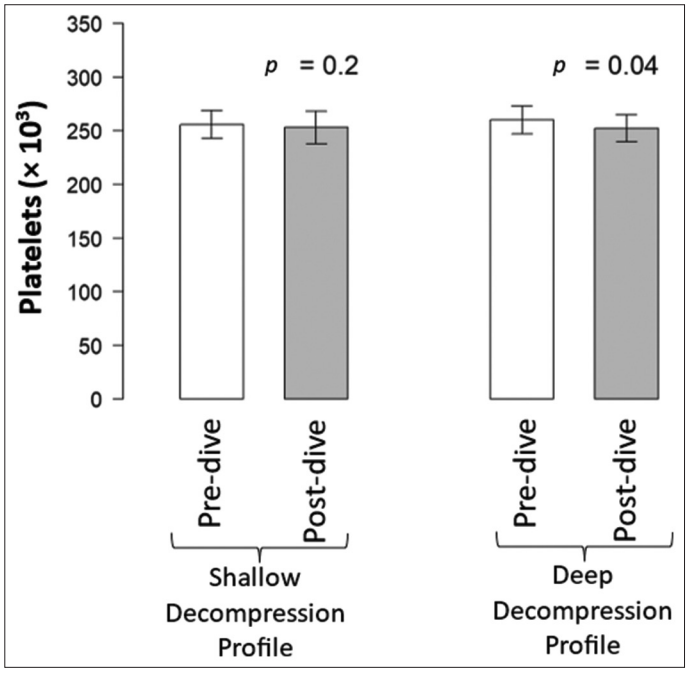

Figure 6. Platelet count (mean ± standard deviation) for the shallow and deep decompression profiles (n = 17). In the shallow decompression profile, the pre-dive mean count was $255 \times 10^3 \pm 54.1 \times 10^3$, and the post-dive mean count was $253 \times 10^3 \pm 52.8 \times 10^3$. In the deep decompression profile, the pre-dive mean count was $260 \times 10^3 \pm 61.5 \times 10^3$, and the post-dive mean count was $252 \times 10^3 \pm 54.4 \times 10^3$

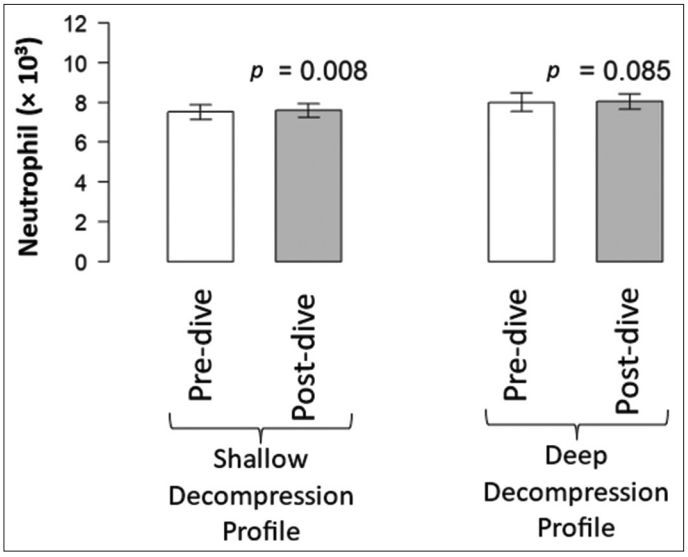

Figure 7. Neutrophil count (mean ± standard deviation) for the shallow and deep decompression profiles (n = 17). In the shallow decompression profile, the pre-dive mean count was $7.512 \times 10^3 \pm 1.56 \times 10^3$, and the post-dive mean count was $8 \times 10^3 \pm 1.90 \times 10^3$. In the Deep Decompression Profile, the pre-dive mean count was $7.594 \times 10^3 \pm 1.36 \times 10^3$, and the post-dive mean count was $8 \times 10^3 \pm 1.55 \times 10^3$

triggered by the sympathetic branch of the ANS. The balance between these opposing forces acts on the vascular smooth muscle cells to maintain vessel tone [36]. The disturbance of

DOI: https://doi.org/10.36922/jctr.24.00021

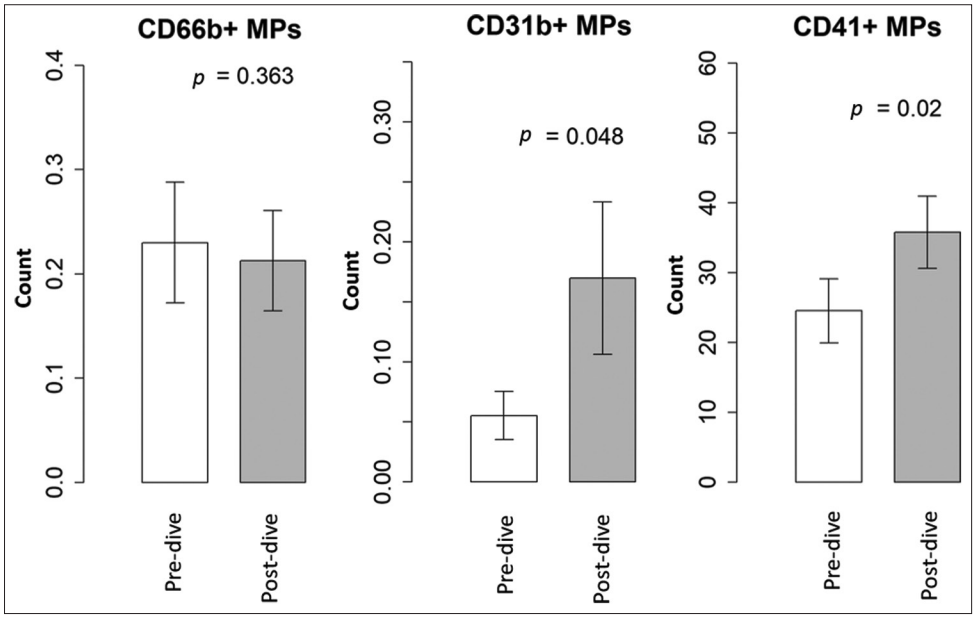

Figure 8. MP count for the deep decompression profile: CD31+ MPs presented a pre-dive mean count of 5.52×10^{-2} and a post-dive mean count of 16.99×10^{-2}; CD41+ MPs presented a pre-dive mean count of 24.5 and a post-dive mean count of 35.8; no significant changes were observed for CD66b+ MPs
Abbreviation: MPs: Microparticles

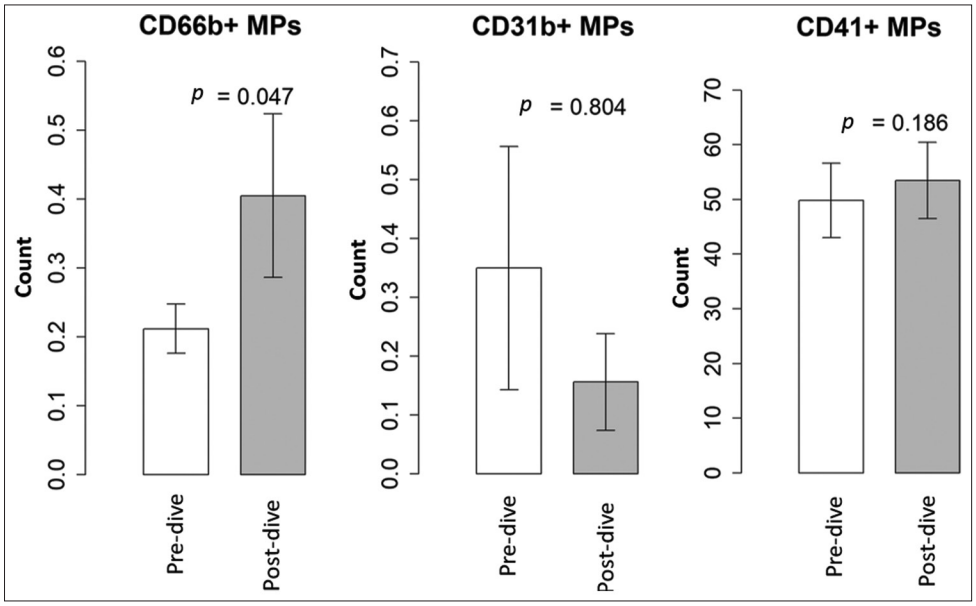

Figure 9. MP count for the shallow decompression profile: CD66b+ MPs presented a pre-dive mean count of 21×10^{-2} and a post-dive mean count of 40×10^{-2}; CD31+ MPs presented a pre-dive mean count of 35×10^{-2} and a post-dive mean count of 15×10^{-2}; CD41+ MPs presented a pre-dive mean count of 49.8 and a post-dive mean count of 53.5
Abbreviation: MPs: Microparticles

this tonic balance, due to the reduced NO availability, maybe the reason why sympathetic activity is associated with loss of endothelial function in some circumstances. Such disturbance of the tonic balance mentioned above is compatible with changes possibly caused by oxidative processes observed in the present study, including the increased numbers of CD31+ MPs [37].

There are also significant increases in HF and RMSSD, variability markers indicating more cardiac control activity. SDNN increased only in the shallow decompression profile. In previous studies, we observed a significant increase in overall HRV in control groups exposed to gases with higher oxygen fractions but not to increased ambient pressure [18].

The results obtained in the present study indicate that different decompression profiles may affect HRV differently, potentially influencing neutrophil count, platelet activation, and MP production. A reduction in circulating platelet counts

DOI: https://doi.org/10.36922/jctr.24.00021

Table 5. MPO and microparticle levels for the deep decompression profile

Parameter	Pre-dive	Post-dive	P
MPO+ (%)	2.448±0.830	2.549±0.888	0.758
MPO (MFI)	576.796±171.399	526.565±137.525	0.472
CD66b+	0.28±0.07	0.27±0.06	0.207
CD31+	0.06±0.03	0.17±0.08	0.022
CD41+	24.50±5.64	35.80±4.92	0.027

Note: Data are presented as mean±standard error.
Abbreviation: MFI: Mean fluorescence intensity; MPO: Myeloperoxidase.

Table 6. MPO and microparticle levels for the shallow decompression profile

Parameter	Pre-dive	Post-dive	P
MPO+ (%)	2.61±1.17	2.32±1.16	0.15
MPO (MFI)	314.95±31.93	291.05±28.29	0.07
CD66b+	0.21±0.04	0.40±0.12	0.000
CD31+	0.35±0.21	0.16±0.08	0.199
CD41+	49.80±6.80	53.46±6.96	0.186

Note: Data are presented as mean±standard error.
Abbreviation: MFI: Mean fluorescence intensity; MPO: Myeloperoxidase.

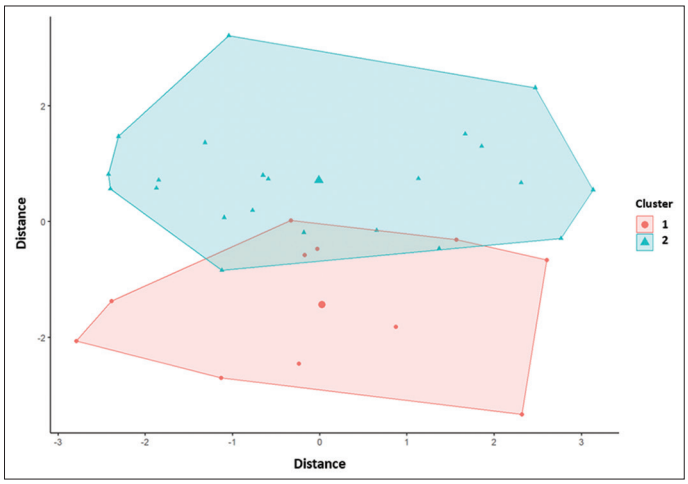

Figure 10. Clusters identified by the clustering algorithm. Cluster 1: Shallow decompression profile; Cluster 2: Deep decompression profile

was observed in the deep decompression profile. Platelets are regarded as effectors of hemostasis, essential for vascular integrity [38,39]. Recent understanding has clarified that they are key effectors in inflammation, immune responses, and signaling, with the potential to orchestrate complex immune and inflammatory events [39,40]. Three different studies by the same research team investigated platelet count and its association with decompression sickness in mice models and with bubble formation in humans [41-43]. Their results indicate that higher bubble counts in humans correlate with a greater reduction in platelet count, even in the absence of decompression sickness after decompression. Conversely, in mice suffering from decompression sickness after provocative decompression, a regression model linked platelet reduction to symptom severity. In both cases, they speculated that such reduction was due to platelet activation and aggregation.

Activated platelets release MPs (CD41 + MPs) that are involved in intercellular (endogenous) signaling by inducing immune responses in distant sites [44]. *In vitro* studies revealed that CD41 + MPs facilitate leukocyte–leukocyte interactions and the binding of P-selectin/P-selectin glycoprotein ligand-1 [45], increasing leukocyte accumulation at injury sites and on activated endothelium. In addition, platelet shedding of MPs positively correlates with increased vascular permeability [46]. The results obtained in this study suggest an increase in circulating CD41+ MPs after decompression in the deep decompression profile, which aligns with the observed reduction in circulating platelets. This is likely due to platelet activation and recruitment to inflammation sites. The release of platelet, endothelial, and leukocyte MPs is increased during inflammatory conditions [13]. Oxidative stress is known to induce the release of CD31+ MPs, which attract leukocytes to the inflammatory site by adhesion molecules, such as vascular cell adhesion molecule-1, a key factor endothelial dysfunction [28,37].

Our results demonstrated a post-dive increase in platelet- and endothelial-derived MPs (CD41+ and CD31+ MPs, respectively) in the deep decompression profile (Figure 9). Similarly, the shallow decompression profile displayed a marked increase in neutrophil-derived MPs (Figure 9).

A decrease in red blood cells and hemoglobin was observed in the deep decompression profile (Figures 4 and 5, respectively), likely due to eryptosis [47,48], a form of programmed cell death in erythrocytes. Eryptosis, triggered by oxidative stress, involves the activation of caspases expressed by erythrocytes, resulting in their recognition and engulfment by circulating macrophages. Since erythrocyte membranes are highly vulnerable to oxidative damage and cannot repair damaged proteins by re-synthesis, they are particularly sensitive to oxidative stress [49]. Eryptosis of young red blood cells is often reported in subjects returning from high altitudes or space flights [47], and its putative mechanism is related to changes in the erythropoietin sensitivity of the cells. Therefore, the observed change in red blood cell and hemoglobin counts might be related to a stressful decompression profile.

The shallow and deep decompression profiles can also be distinguished by indicators of immune system activation and inflammation. The shallow decompression profile increases peripheral blood neutrophil count and its corresponding MPs, without affecting platelet count and its MPs, as well as in endothelial MPs. Conversely, the deep decompression profile exhibited an increase in the platelet- and endothelial-derived MPs and a decrease in platelet count, with no variations in neutrophil count and its MPs.

Neutrophils are widely recognized for their role in promoting inflammatory responses at the initial stages of these processes. Increased neutrophil count is associated with various pathologies (e.g., bacterial infections, hypertension, and certain types of cancer [50-54]) and non-pathological conditions (e.g., after exercising) [55]. Their activation might also promote platelet activation [13,44] and even endothelial damage [13,56], then

DOI: https://doi.org/10.36922/jctr.24.00021

enhancing the inflammatory process. From this more orthodox standpoint, increased neutrophil count and activation would act as pro-inflammatory agents.

However, neutrophils play an anti-inflammatory role in many instances. Neutrophil-derived MPs are potential inhibitors of macrophage activation [57]. For instance, annexin-1-rich neutrophil-derived MPs inhibit neutrophil activation [58], downregulating an inflammatory response. The production of platelet activation factors depends on the neutrophils' state; it occurs when neutrophils are adherent (i.e., under a stimulated condition) but not when they are in suspension [44]. Neutrophil-derived MPs are not a homogeneous set, and they can induce or inhibit inflammation [59]. Besides this functional diversity, variations in neutrophil counts might lead to different outcomes. For instance, an increase in neutrophil count seems to be associated with benign prostate enlargement, whereas a decrease might indicate a malignant case [60]. Exercise-induced neutrophilia illustrates the challenge of defining a consistent pattern in response to physical effort, as reports of neutrophil counts in peripheral blood vary widely. In our previous study [19], the MPO MFI, an important marker of neutrophil activation, demonstrated a negative correlation with the number of circulating neutrophils (−0.55), and a significant positive correlation with the percentage of granulocytes expressing MPO on the membrane surface (0.7). A negative correlation between neutrophil-derived MPs (CD66b+) and MPO MFI was also observed (−0.32). These results suggest that increased circulating neutrophil counts are not necessarily indicative of their activation or associated inflammatory processes.

It is also important to consider the role of platelet- and endothelial-derived MPs and their interactions with neutrophils. Platelets, once regarded as a thrombus-forming agent, are now recognized as primary players in inflammatory processes. Activated platelets produce platelet-derived MPs that induce neutrophil clustering and further activation [45,61]. Similarly, endothelial-derived MPs induce neutrophil adhesion and activation [62]. Therefore, an inflammatory process can become self-sustaining, as the activation of one cell type leads to the activation of another, which in turn further activates the original cell type. In such a setting, an intriguing phenomenon may occur: Despite being activated and having a tendency for neutrophilia, the neutrophil count might decrease due to migration/sequestration in damaged tissues [63,64]. In other words, the inflammatory condition might appear, without changes in neutrophil count.

Considering HRV as an index of physiological stress from various sources, our results, along with other reports [18,32], suggest the putative illustration depicted in Figure 10. The initial phase of decompression leads to a certain degree of bubble formation and inflammatory response activation [65]. Subsequently, depending on the decompression rate, one of three outcomes may occur, as modeled in a dynamical system by Schirato *et al.* [65], which represent the interactions of supersaturation, bubble production, inflammation, and their respective feedbacks.

In the case of elevated overall supersaturation, increased tissue damage and bubble formation occur, resulting in positive inflammatory feedback [66,67]. At the end of the decompression process, a state of high physiological stress with an important inflammatory process in progress is likely to be observed. In this case, subjects will most probably develop decompression sickness [68].

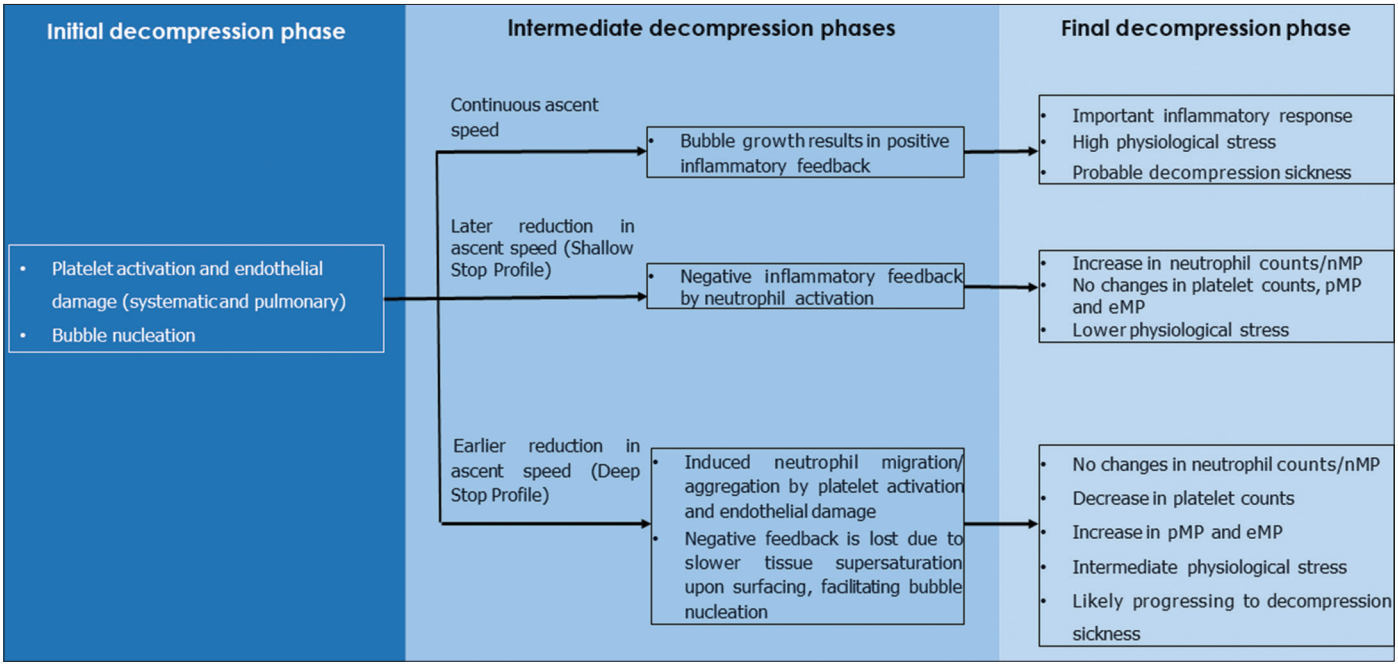

Figure 11. Possible schematics of the immune system response to decompression, with platelet- and endothelial-derived MPs are referred to as pMPs and eMPs, respectively
Abbreviation: MP: Microparticle; pMPs: Platelet microparticles; eMPs: Endothelial microparticles

DOI: https://doi.org/10.36922/jctr.24.00021

Finally, if the decompression proceeds at a pace that allows neutrophils to become active but not activated by platelet- and endothelial-derived MPs, they will inhibit the ongoing inflammatory process initiated earlier. Bubble formation would likely be minimal due to the absence of nucleation sources, resulting in the individual surfacing with low physiological stress.

The levels of supersaturation required to trigger the processes depend on individual responses, i.e., activation of the person's inflammatory processes. Moreover, the correlation between HRV and the degree of stress (sympathetic tonus) seems to be highly individualized. Notably, different decompression profiles generate different tissue supersaturation upon surfacing. The composition of the breathing gases (i.e., the fraction of oxygen and the presence of helium) causes different physiological responses. It might be possible to speculate the existence of a dose-dependent response, where lower tissue supersaturation would lead to little or no physiological alterations, while higher tissue supersaturations would lead to progressively greater physiological responses and subsequently the development of decompression sickness.

Our proposed schematics presented in Figure 11 highlight two aspects of decompression: (i) the combination of bubble count, inflammatory markers, and HRV can be an important predictor of decompression success on an individual basis; (ii) if a clear relationship between HRV indexes and bubble/inflammation is established post-decompression, HRV could be employed to assess an individual's likelihood of success in a given decompression profile.

Of course, the ideas presented in this study should be interpreted with caution due to the small cohort of investigated divers and the large inter-individual variance observed in the variables analyzed. Besides, it is important to note that the data were obtained through dives simulated in hyperbaric chambers, which might not necessarily reflect the actual conditions encountered when divers are immersed [69], though the data obtained in chamber and swimming pool dives, already presented in other studies, displayed similar patterns.

5. Conclusion

Although no cases of decompression sickness were observed in the experiments described in this manuscript, it has been demonstrated in the present study that different decompression profiles trigger different physiological responses. Whether these physiological responses translate into a higher risk of developing symptoms of decompression sickness is unclear at the present moment, and further research is required. It can be speculated, however, that, according to the scheme described in Figure 11 and further developed by Schirato *et al.* [65], they might play a relevant role in more aggressive exposures.

Acknowledgments

None.

Funding

None.

Conflicts of Interest

The authors have no competing interests.

Ethics Approval and Consent to Participate

The volunteers provided written informed consent. The ethical committee of the Biosciences Institute of the University of Sao Paulo approved the experimental protocol (CAE #91231618.6.0000.5464), and all experiments were performed in accordance with relevant guidelines and regulations.

Consent for Publication

All volunteers signed an informed consent before joining the experiments.

Availability of Data

Data are available from the corresponding author upon reasonable request.

References

[1] Boycott AE, Damant GC, Haldane JS. The Prevention of Compressed-air Illness. J Hyg (Lond) 1908;8:342-443. doi: 10.1017/s0022172400003399

[2] Bühlmann A. Decompression, Decompression Sickness. Berlin: Springer Verlag Heidelberg; 1984. doi: 10.1007/978-3-662-02409-6

[3] Howle LE, Weber PW, Hada EA, Vann RD, Denoble PJ. The Probability and Severity of Decompression Sickness. PLoS One 2017;12(3):1-25. doi: 10.1371/journal.pone.0172665

[4] Doolette D, Gerth W, Gault K. Redistribution of Decompression Stop Time from Shallow to Deep Stops Increases Incidence of Decompression Sickness in Air Decompression Dives. Panama City: Navy Experimental Diving Unit; 2011.

[5] Yount DE, Hoffman DC. On the Use of a Bubble Formation Model to Calculate Diving Tables. Aviat Space Environ Med 1986;57:149-56.

[6] Marroni A, Bennett PB, Cronje FJ, Cali-Corleo R, Germonpre P, Pieri M, *et al*. A Deep Stop during Decompression from 82 fsw (25 m) Significantly Reduces Bubbles and Fast Tissue Gas Tensions. Undersea Hyperb Med 2004;31:233-43.

[7] Doolette DJ. Venous Gas Emboli Detected by Two-Dimensional Echocardiography are an Imperfect Surrogate Endpoint for Decompression Sickness. Diving Hyperb Med 2016;46:4-10.

[8] Doolette DJ, Murphy FG, Gerth WA. Thalmann Algorithm parameter sets for support of constant 1.3 atm PO_2 He-O_2 diving to 300 fsw. Panama City:Navy Experimental Diving Unit; 2018.

[9] Madden LA, Laden G. Gas Bubbles may not be the Underlying cause of Decompression Illness - the at-

Depth Endothelial Dysfunction Hypothesis. Med Hypotheses 2009;72:389-92.
doi: 10.1016/j.mehy.2008.11.022

[10] Thom SR, Bennett M, Banham ND, Chin W, Blake DF, Rosen A, *et al*. Association of Microparticles and Neutrophil Activation with Decompression Sickness. J Appl Physiol 2015;119:427-34.
doi: 10.1152/japplphysiol.00380.2015

[11] Bhullar J, Bhopale VM, Yang M, Sethuraman K, ThomSR. Microparticle Formation by Platelets Exposed to High Gas Pressures - An Oxidative Stress Response. Free Radic Biol Med 2016;101:154-62.
doi: 10.1016/j.freeradbiomed.2016.10.010

[12] Batool S, Abbasian N, Burton JO, Stover C. Microparticles and their Roles in Inflammation: A Review. Open Immunol J 2013;6:1-14.
doi: 10.2174/1874226201306010001

[13] Cognasse F, Hamzeh-Cognasse H, Laradi S, ChouML, Seghatchian J, Burnouf T, *et al*. The Role of Microparticles in Inflammation and Transfusion: A Concise Review. Transfus Apher Sci 2015;53:159-67.
doi: 10.1016/j.transci.2015.10.013

[14] Puddu P, Puddu GM, Cravero E, Muscari S, Muscari A. The Involvement of Circulating Microparticles in Inflammation, Coagulation and Cardiovascular Diseases. Can J Cardiol 2010;26:140-5.
doi: 10.1016/S0828-282X(10)70371-8

[15] Brett KD, Nugent NZ, Fraser NK, Bhopale VM, Yang M, Thom SR. Microparticle and Interleukin-1B Production with Human Simulated Compressed Air Diving. Sci Rep 2019;9:13320.

[16] Thom SR, Bhopale VM, Yang M. Neutrophils Generate Microparticles during Exposure to Inert Gases Due to Cytoskeletal Oxidative Stress. J Biol Chem 2014;289:18831-45.
doi: 10.1074/jbc.M113.543702

[17] Winterbourn CC, Kettle AJ, Hampton MB. Reactive Oxygen Species and Neutrophil Function. Annu Rev Biochem 2016;85:765-92.
doi: 10.1146/annurev-biochem-060815-014442

[18] Schirato SR, El-Dash I, El-Dash V, Natali JE, Starzynski PN, Chaui-Berlinck JG. Heart Rate Variability Changes as an Indicator of Decompression-Related Physiological Stress. Undersea Hyperb Med 2018;45:173-82.

[19. Schirato SR, El-Dash I, El-Dash V, Bizzarro B, Marroni A, Pieri M, *et al*. Association between Heart Rate Variability and Physiological Stress. Front Physiol 2020;11:743.
doi: 10.3389/fphys.2020.00743

[20] The North American, Task Force of the European Society of Cardiology and The North American Society of Pacing and Electrophysiology. Heart Rate Variability: Standards of Measurement, Physiological Interpretation, and Clinical Use. Eur Heart J 1996;17:354-81.
doi: 10.1161/01.CIR.93.5.1043

[21] von Käne R, Nelesen RA, Mills PJ, Ziegler MG, Dimsdale JE. Relationship between Heart Rate Variability, Interleukin-6, and Soluble Tissue Factor in Healthy Subjects. Brain Behav Immun 2008;22:461-8.

[22] Kaufman CL, Kaiser DR, Steinberger J, Dengel DR. Relationships between Heart Rate Variability, Vascular Function, and Adiposity in Children. Clin Auton Res 2007;17:165-71.
doi: 10.1007/s10286-007-0411-6

[23] Haraguchi R, Hoshi H, Ichikawa S, Hanyu M, Nakamura K, Fukasawa K, *et al*. The Menstrual Cycle Alters Resting-State Cortical Activity: A Magnetoencephalography Study. Front Hum Neurosci 2021;15:652789.
doi: 10.3389/fnhum.2021.652789

[24] Cialoni D, Pieri M, Balestra C, Marroni A. Dive Risk Factors, Gas Bubble Formation, and Decompression Illness in Recreational SCUBA Diving: Analysis of DAN Europe DSL Data Base. Front Psychol 2017;8:1587.
doi: 10.3389/fpsyg.2017.01587

[25] Thom SR, Yang M, Bhopale VM, Milovanova TN, Bogush M, Buerk DG. Intramicroparticle Nitrogen Dioxide is a Bubble Nucleation Site Leading to Decompression-Induced Neutrophil Activation and Vascular Injury. J Appl Physiol 2013;114:550-8.
doi: 10.1152/japplphysiol.01386.2012

[26] Thom SR, Milovanova TN, Bogush M, Bhopale VM, Yang M, Bushmann K, *et al*. Microparticle Production, Neutrophil Activation, and Intravascular Bubbles Following Open-Water SCUBA Diving. J Appl Physiol 2012;112:1268-78.
doi: 10.1152/japplphysiol.01305.2011

[27] Ludbrook J, Dudley H. Why Permutation Tests Are Superior to t and F Tests in Biomedical Research. John Ludbrook and Hugh Dudley Source : The American Statistician, 52, 127-132. Am Stat Assoc 2008;52:127-32.

[28] Vince RV, McNaughton LR, Taylor L, Midgley AW, Laden G, Madden LA. Release of VCAM-1 Associated Endothelial Microparticles Following Simulated SCUBA Dives. Eur J Appl Physiol 2009;105:507-13.
doi: 10.1007/s00421-008-0927-z

[29] Madden D, Thom SR, Dujic Z. Exercise Before and After SCUBA Diving and the Role of Cellular Microparticles in Decompression Stress. Med Hypotheses 2016;86:80-4.
doi: 10.1016/j.mehy.2015.12.006

[30] Ernst G. Heart-Rate Variability-More than Heart Beats? Front Public Health 2017;5:240.
doi: 10.3389/fpubh.2017.00240

[31] Noh Y, Posada-Quintero HF, Bai Y, White J, Florian JP,

Brink PR, *et al*. Effect of Shallow and Deep SCUBA Dives on Heart Rate Variability. Front Physiol 2018;9:110.
doi: 10.3389/fphys.2018.00110

[32] Marchitto N, Iannarelli N, Paparello PT, Cioeta E, Parisi F, Pirrone S, *et al*. The Cardiovascular Risk in the Scuba Divers. J Sports Med Phys Fitness 2019;59:1779-82.
doi: 10.23736/S0022-4707.19.09358-7

[33] Lauscher P, Kertscho H, Enselmann P, Lauscher S, Habler O, Meier J. Effects of Alterations of Inspiratory Oxygen Fractions on Heart Rate Variability. Br J Anaesth 2012;108:402-8.
doi: 10.1093/bja/aer404

[34] Chapleau MW, Li Z, Meyrelles SS, Ma X, Abboud FM. Mechanisms Determining Sensitivity of Baroreceptor Afferents in Health and Disease. Ann N Y Acad Sci 2006;940:1-19.
doi: 10.1111/j.1749-6632.2001.tb03662.x

[35] Rahman F, Pechnik S, Gross D, Sewell L, Goldstein DS. Low Frequency Power of Heart Rate Variability Reflects Baroreflex Function, not Cardiac Sympathetic Innervation. Clin Auton Res 2011;21:133-41.
doi: 10.1007/s10286-010-0098-y

[36] Harris KF, Matthews KA. Interactions between Autonomic Nervous System Activity and Endothelial Function: A Model for the Development of Cardiovascular Disease. Psychosom Med 2004;66:153-64.
doi: 10.1097/01.psy.0000116719.95524.e2

[37] Brodsky SV, Zhang F, Nasjletti A, Goligorsky MS. Endothelium-Derived Microparticles Impair Endothelial Function *in Vitro*. Am J Physiol Heart Circ Physiol 2004;286(5):H1910-5.
doi: 10.1152/ajpheart.01172.2003

[38] Cialoni D, Brizzolari A, Barassi A, Bosco G, Pieri M, Lancellotti V, *et al*. White Blood Cells, Platelets, Red Blood Cells and Gas Bubbles in SCUBA Diving: Is there a Relationship? Healthcare (Basel) 2022;10:182.
doi: 10.3390/healthcare10020182

[39] Lindemann S, Tolley ND, Dixon DA, McIntyre TM, Prescott SM, Zimmerman GA, *et al*. Activated Platelets Mediate Inflammatory Signaling by Regulated Interleukin 1β Synthesis. J Cell Biol 2001;154:485-90.
doi: 10.1083/jcb.200105058

[40] Alicia P, Yourish K. Platelets: Versatile Effector Cells in Hemostasis, Inflammation, and the Immune Continuum. Nyt 2018;34:5-30.
doi: 10.1007/s00281-011-0286-4

[41] Pontier JM, Vallée N, Bourdon L. Bubble-Induced Platelet Aggregation in a Rat Model of Decompression Sickness. J Appl Physiol (1985) 2009;107:1825-9.
doi: 10.1152/japplphysiol.91644.2008

[42] Pontier JM, Blatteau JE, Vallée N. Blood Platelet Count and Severity of Decompression Sickness in Rats After a Provocative Dive. Aviat Space Environ Med 2008;79:761-4.
doi: 10.3357/ASEM.2299.2008

[43] Pontier JM, Jimenez C, Blatteau JE. Blood Platelet Count and Bubble Formation After a Dive to 30 msw for 30 Min. Aviat Space Environ Med 2008;79:1096-9.
doi: 10.3357/ASEM.2352.2008

[44] Watanabe J, Marathe GK, Neilsen PO, Weyrich AS, Harrison KA, Murphy RC, *et al*. Endotoxins Stimulate Neutrophil Adhesion Followed by Synthesis and Release of Platelet-Activating Factor in Microparticles. J Biol Chem 2003;278:33161-8.
doi: 10.1074/jbc.M305321200

[45] Jy W, Mao WW, Horstman LL, Tao J, Ahn YS. Platelet Microparticles Bind, Activate and Aggregate Neutrophils *in Vitro*. Blood Cells Mol Dis. 1995;21:217-31.
doi: 10.1006/bcmd.1995.0025

[46] Hottz ED, Lopes JF, Freitas C, Valls-de-Souza R, Oliveira MF, Bozza MT, *et al*. Platelets Mediate Increased Endothelium Permeability in Dengue through NLRP3-Inflammasome Activation. Blood 2013;122:3405-14.
doi: 10.1182/blood-2013-05-504449

[47] Lang F, Lang E, Fller M. Physiology and Pathophysiology of Eryptosis. Transfus Med Hemother 2012;39:308-14.
doi: 10.1159/000342534

[48] Pretorius E, Du Plooy JN, Bester J. A Comprehensive Review on Eryptosis. Cell Physiol Biochem 2016;39:1977-2000.
doi: 10.1159/000447895

[49] Perovic A, Nikolac N, Njire Braticevic M, Milcic A, Sobocanec S, Balog T, *et al*. Does Recreational Scuba Diving have Clinically Significant Effect on Routine Haematological Parameters? Biochem Med (Zagreb) 2017;27:27-38.
doi: 10.11613/BM.2017.035

[50] Al-Gwaiz LA, Babay HH. The Diagnostic Value of Absolute Neutrophil Count, Band Count and Morphologic Changes of Neutrophils in Predicting Bacterial Infections. Med Princ Pract 2007;16:344-7.
doi: 10.1159/000104806

[51] Tatsukawa Y, Hsu WL, Yamada M, Cologne JB, Suzuki G, Yamamoto H, *et al*. White Blood Cell Count, Especially Neutrophil Count, as a Predictor of Hypertension in a Japanese Population. Hypertens Res 2008;31:1391-7.
doi: 10.1291/hypres.31.1391

[52] de Jager CPC, Wever PC, Gemen EFA, Kusters R, van Gageldonk-Lafeber AB, van der Poll T, *et al*. The Neutrophil-Lymphocyte Count Ratio in Patients with Community-Acquired Pneumonia. PLoS One 2012;7:e46561.
doi: 10.1371/journal.pone.0046561

[53] Teramukai S, Kitano T, Kishida Y, Kawahara M,

Kubota K, Komuta K, *et al*. Pretreatment Neutrophil Count as an Independent Prognostic Factor in Advanced Non-Small-Cell Lung Cancer: An Analysis of Japan Multinational Trial Organisation LC00-03. Eur J Cancer 2009;45:1950-8.
doi: 10.1016/j.ejca.2009.01.023

[54] Shafi S, Afsheen M, Reshi F. Total Leucocyte Count, C-Reactive Protein and Neutrophil Count: Diagnostic Aid in Acute Appendicitis. Saudi J Gastroenterol 2009;15:117.
doi: 10.4103/1319-3767.48969

[55] Peake J, Suzuki K. Neutrophil Activation, Antioxidant Supplements and Exercise-Induced Oxidative Stress. Exerc Immunol Rev 2004;10:129-41.

[56] Pitanga TN, de Aragão França L, Rocha VCJ, Meirelles T, Borges VM, Gonçalves MS, *et al*. Neutrophil-Derived Microparticles Induce Myeloperoxidase-Mediated Damage of Vascular Endothelial Cells. BMC Cell Biol 2014;15:21.
doi: 10.1186/1471-2121-15-21

[57] Gasser O, Schifferli JA. Activated Polymorphonuclear Neutrophils Disseminate Anti-Inflammatory Microparticles by Ectocytosis. Blood 2004;104:2543-8.
doi: 10.1182/blood-2004-01-0361

[58] Dalli J, Norling LV, Renshaw D, Cooper D, Leung KY, Perretti M. Annexin 1 Mediates the Rapid Anti-Inflammatory Effects of Neutrophil-Derived Microparticles. Blood 2008;112:2512-9.
doi: 10.1182/blood-2008-02-140533

[59] Dalli J, Montero-Melendez T, Norling LV, Yin X, Hinds C, Haskard D, *et al*. Heterogeneity in Neutrophil Microparticles Reveals Distinct Proteome and Functional Properties. Mol Cell Proteomics 2013;12:2205-19.
doi: 10.1074/mcp.M113.028589

[60] Fujita K, Imamura R, Tanigawa G, Nakagawa M, Hayashi T, Kishimoto N, *et al*. Low Serum Neutrophil Count Predicts a Positive Prostate Biopsy. Prostate Cancer Prostatic Dis 2012;15:386-90.
doi: 10.1038/pcan.2012.27

[61] Maugeri N, Capobianco A, Rovere-Querini P, Ramirez GA, Tombetti E, Valle PD, *et al*. Platelet Microparticles Sustain Autophagy-Associated Activation of Neutrophils in Systemic Sclerosis. Sci Transl Med 2018;10:eaao3089.
doi: 10.1126/scitranslmed.aao3089

[62] Buesing KL, Densmore JC, Kaul S, Pritchard KA Jr., Jarzembowski JA, Gourlay DM, *et al*. Endothelial Microparticles Induce Inflammation in Acute Lung Injury. J Surg Res 2011;166:32-9.
doi: 10.1016/j.jss.2010.05.036

[63] Lee WL, Downey GP. Neutrophil Activation and Acute Lung Injury. Curr Opin Crit Care 2001;7:1-7.
doi: 10.1097/00075198-200102000-00001

[64] Nakagawa M, Toy P. Related Acute Lung Injury : Cases at One Hospital. Transfusion (Paris) 2004;44:1689-94.

[65] Schirato SR, Silva V, Iadocicco K, Maronni A, Pieri M, Cialoni D, *et al*. Post-Decompression Bubble and Inflammation Interactions: A Non-extensive Dynamical System Model. Undersea Hyperb Med 2022;49:207-26.
doi: 10.22462/03.04.2022.6

[66] Thom SR, Milovanova TN, Bogush M, Yang M, Bhopale VM, Pollock NW, *et al*. Bubbles, Microparticles, and Neutrophil Activation: Changes with Exercise Level and Breathing Gas During Open-Water SCUBA Diving. J Appl Physiol 2013;114:1396-405.
doi: 10.1152/japplphysiol.00106.2013

[67] Zhang K, Wang D, Jiang Z, Ning X, Buzzacott P, Xu W. Endothelial Dysfunction Correlates with Decompression Bubbles in Rats. Sci Rep 2016;6:33390.
doi: 10.1038/srep33390

[68] Imbert JP, Egi SM, Germonpré P, Balestra C. Static Metabolic Bubbles as Precursors of Vascular Gas Emboli During Divers' Decompression: A Hypothesis Explaining Bubbling Variability. Front Physiol 2019;10:807.
doi: 10.3389/fphys.2019.00807

[69] Vann RD, Gerth WA, Denoble PJ, Pieper CF, Thalmann ED. Experimental Trials to Assess the Risks of Decompression Sickness in Flying After Diving. UHM 2004;31:431-44.

DOI: https://doi.org/10.36922/jctr.24.00021